High heat resistant front-end XY slit at SPing-8

Mutsumi Sano[1)]
1)Japan Synchrotron Radiation Research Institute (JASRI)
1-1-1 Kouto Sayo-cho Sayo-gun, Hyogo 679-5198, Japan

Sunao Takahasi[1)], **Atsuo Watanabe**[1)], **Hideo Kitamura**[1),2)]
2) RIKEN SPring-8 Center
1-1-1 Kouto Sayo-cho Sayo-gun, Hyogo 679-5148, Japan

Abstract:

The thermal contact conductance (TCC) of a high heat resistant front-end XY slit was estimated in order to predict the maximum temperature. We were able to obtain the minimum TCC by comparing the results of an experiment with those of a finiteelement method analysis. The maximum temperature of the XY slit was calculated by applying the minimum TCC.

1-Introduction

At SPring-8, a front end XY slit, which is used to eliminate the unwanted part of the synchrotron radiation (SR) to reduce the heat load on downstream components, is being upgraded to give it high heat resistance. It consists of a heat-absorbing part made of GlidCop and a beam-forming part made of tantalum (Ta slit), both of which are attached with bolts. The Ta slit of the conventional XY slit receives SR at a normal incidence with an indirect cooling geometry. Because the advancement of the insertion device has resulted in a progressive increase in the heat load, we needed to pay attention to improving the heat resistance of both the absorbing part and the Ta slit. As a result, a high heat resistant (HHR) XY slit was proposed, whose Ta slit receives SR at an inclined incidence in order to reduce the effective power density. Accurate estimation of the thermal contact conductance (TCC) between the absorbing part and the Ta slit is crucial for precisely predicting the maximum temperature. The TCC was estimated by consolidating the results of experiments and finite element method (FEM) analyses. These procedures were the same as those used in a previous study [1]. The experiments were carried out using specially designed small test pieces, which had the same configuration and contact surface conditions as those of an actual XY slit. The temperature drops between the absorbing part and the Ta slit, which was heated using an electron beam, were measured near the interface. Although the TCC is influenced by many factors, we focused on fastening torque and interstitial materials as the influencing factors in this experiment. The TCCs were examined for both the HHR XY slit and the conventional XY slit.

2-Experiment

Figs. 1(a) and 1(b) show the conventional and HHR XY slit test pieces, respectively. Each test piece consisted of a cooling part made of GlidCop and the Ta slit, which were connected using three bolts (size M3). Two holes for embedding the thermocouples were manufactured in the interface. An electron beam was used to irradiate the marked area of the Ta slit shown in Fig. 1. A slit with a 3 mm aperture was installed on the upstream side of the Ta slit in order to restrict the absorbing area. Table 1 lists the experimental conditions for each test piece. Although the actual torque used in the assembly of the XY slit is 1.4 N·m, we also examined the results when using a smaller torque. The actual input power was calculated from the flow rate and the temperature difference between the inlet and the outlet of the cooling water.

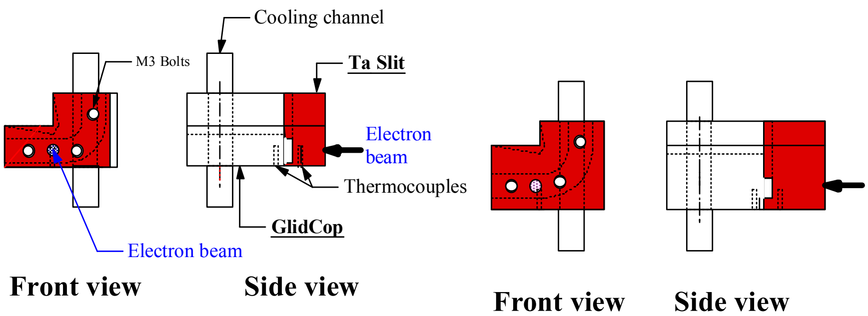

(a) Conventional XY slit (b) HHR XY slit

Figure 1 Schematic drawings of test pieces of the XY slit.

Table 1 Experimental conditions.

	Conventional XY slit	**HHR XY slit**
Interstitial material	50- m-thick Ag, no material	50- m-thick Ag, no material
Fastening torque	0.63 N·m, 1.4 N·m	1.4 N·m
Absorbed power	50 W	50 W
Flow rate of the cooling water	3 L/min	3 L/min

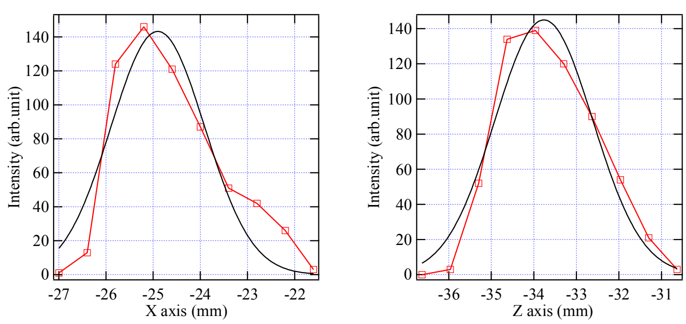

(a) Horizontal direction (b) Vertical direction

Figure 2 Electron beam profiles in horizontal and vertical directions.

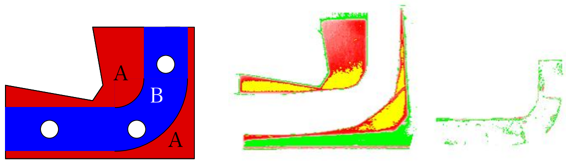

(a) Contact area(b) Pressure distributions of area A and area B

Figure 3 Contact area and pressure distribution for conventional XY slit.

(a) Contact area (b) Pressure distributions of area A and area B

Figure 4 Contact area and pressure distribution for HHR XY slit.

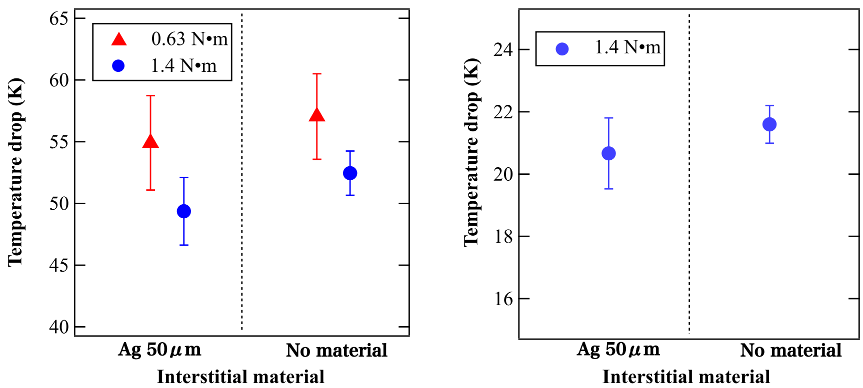

(a) Conventional XY slit (b) HHR XY slit

Figure 5 Relationships between interstitial material and temperature drop.

Figs. 2(a) and 2(b) show the electron beam profiles in the horizontal and vertical directions, respectively. The solid lines indicate the fitting results by Gaussian functions. These results were applied to the boundary conditions of the FEM analysis. In order to define the TCC of the interface, the contact pressure of the interface was measured, because the contact area had to be divided into two areas (area A and area B) whether the interstitial material was inserted or not. In the case of the actual XY slit, the 50- m-thick Ag foil is inserted in area A, whereas area B is no interstitial material. According to the actual XY slit, the interstitial material is inserted in only area A in this study. Figs. 3 and 4 show the contact area and pressure distribution, respectively, of the interface for a fastening torque of 1.4 N·m for each test piece. As a result, the average contact pressures of area A and area B were 50 MPa and 0.12 MPa for the conventional type and 20 MPa and 0.2 MPa for the HHR type, respectively.Figs. 5(a) and 5(b) show the experimental results of the relationships between the interstitial material and the temperature drop for the test pieces of the conventional XY slit and HHR XY slit, respectively. The experiments were carried out about 10 times for each condition, and the test piece was re-assembled for each experiment. The marks and error bars indicate the average values and standard deviations, respectively. For each setup of the test piece, the average temperature drop with the 50- m-thick Ag foil was smaller than that without any interstitial material. These results indicate that Ag foil is effective in improving the contact condition. A comparison of the temperature drops for the conventional type with those for the HHR type shows that the values for the HHR type were smaller than those for the conventional type. This result indicates that the configuration of the HHR XY slit decreases the heat load of the Ta slit.

2-FEM analyses

We conducted thermal analyses using the finite-element program ANSYS. A surface-to-surface contact element, by which the TCC could be defined directly, was placed on the interface. According to the pressure measurements, the pressure ratios of area A to area B were 400:1 for the conventional type and 100:1 for the HHR type. We assumed that each TCC was proportional to the pressure ratio. Table 2 presents the boundary condition used for the FEM analysis. Figs. 6(a) and 6(b) show examples of the temperature distributions acquired from the nodal solutions. The temperature drop between GlidCop and the Ta slit for each TCC was calculated from the nodal solutions corresponding to actual thermocouple locations. Figs. 7(a) and 7(b) show the relationships between the various TCCs of area A and the temperature drops at the actual thermocouple locations. Accordingly, the actual TCCs could be assumed from the temperature drops observed in the experiments.

Table 2 Boundary conditions of FEM analysis.

	Conventional XY slit	**HHR XY slit**
Absorbed power	50 W	
Area of absorbed power	3 mm	
Heat transfer coefficient	9200 $W \cdot m^{-2} \cdot K^{-1}$	
Water temperature	30 °C	
TCC of area A	10,000~600,000 $W \cdot m^{-2} \cdot K^{-1}$	100,000~1,000,000 $W \cdot m^{-2} \cdot K^{-1}$
TCC of area B	25~1500 $W \cdot m^{-2} \cdot K^{-1}$	1000~10,000 $W \cdot m^{-2} \cdot K^{-1}$

Figs. 8(a) and 8(b) show the TCCs for each interstitial material and fastening torque, which were estimated from the experimental results. The symbols and error bars indicate the average values and standard deviations, respectively. It is apparent that for every setup of the test piece, the average TCC value for the 50-

m-thick Ag foil was larger than that without interstitial material. In contrast, the error bars in the case without interstitial material are smaller than those for the 50- m-thick Ag foils. In the case of the conventional XY slit, the average TCCs for the fastening torque of 1.4 N·m were more than double those for the fastening torque of 0.63 N·m. As a result, considering the error bars, we could expect that the minimum TCCs of area A for the conventional XY slit were 80,000 W·m^{-2}·K^{-1} for the fastening torque of 0.63 N·m and 150,000 W·m^{-2}·K^{-1} for that of 1.4 N·m, while the minimum TCC for the HHR XY slit was 400,000 W·m^{-2}·K^{-1}.

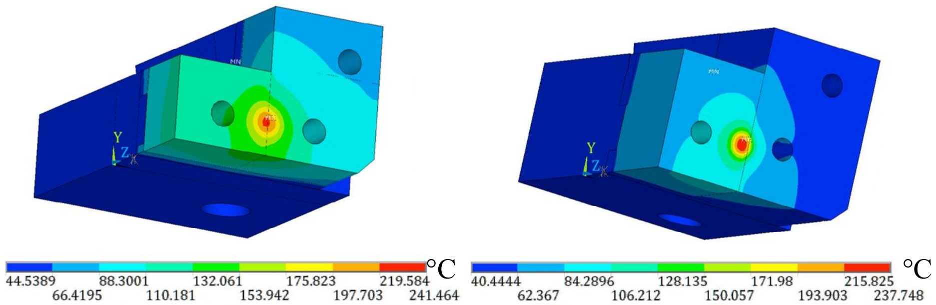

(a) Conventional XY slit (b) HHR XY slit

Figure 6 Temperature distributions from nodal solutions.

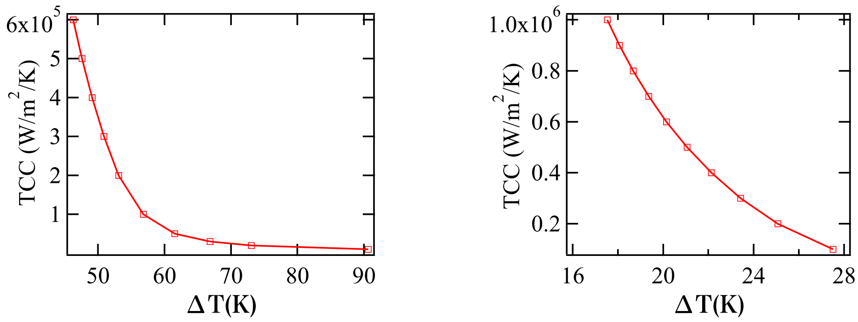

(a) Conventional XY slit (b) HHR XY slit

Figure 7 Relationship between TCC and temperature difference at actual thermocouple locations.

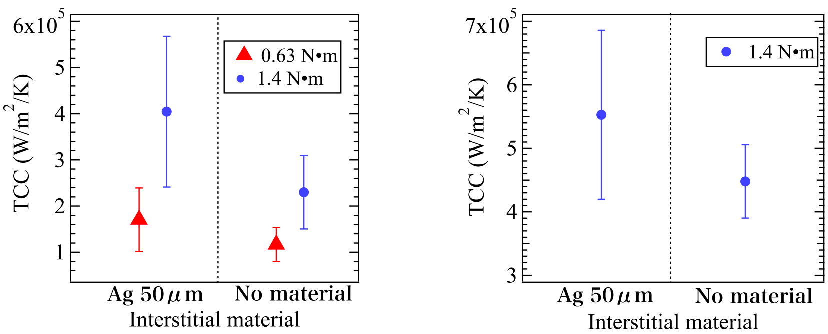

(a) Conventional XY slit (b) HHR XY slit

Figure 8 TCCs for each interstitial material and fastening torque.

3-Evaluation of maximum temperature

The obtained results were applied to a preliminary thermal analysis of the maximum heat load of the Ta slit using the test pieces. We chose BL37XU and BL43LXU as the beamlines for installing the conventional XY slit and HHR XY slit, respectively. BL37XU is the standard undulatorbeamline, whereas BL43LXU is the long undulatorbeamline. The total power values of these beamlines were 13.6 kW and 50.8 kW, respectively. The heat load from BL43LXU is our latest target value. The area for absorbing the power on the Ta slit, which was restricted by the pre-slit, was 4 mm × 0.1 mm for the conventional XY slit. In contrast, this area, which was restricted by the movable mask, was 4 mm × 6 mm for the HHR XY slit. The absorbed power values of the Ta slit for these beamlines were 228 W and 667 W, respectively. The conventional XY slit was heated at a normal incidence, whereas the HHR XY slit was heated at an inclined incidence. The minimum TCCs described above for each condition were applied to the interfaces. The heat transfer coefficient and water temperature were the same as in the above calculations. Figs. 9(a) and 9(b) show the temperature distributions from the nodal solutions.In the case of the conventional XY slit, the maximum temperatures were 2,238 °C for a TCC of 80,000 $W\cdot m^{-2}\cdot K^{-1}$and 2,210 °C for a TCC of 150,000 $W\cdot m^{-2}\cdot K^{-1}$.This means that even if the fastening bolts loosen, the maximum temperature will not increase significantly.In contrast, in the case of the HHR XY slit, the maximum temperature was 1,863 °C.On the other hand the maximum temperatures of absorbing part made of GlidCop were 202 °C for the conventional XY slit and 321 °C for the HHR XY slit, respectively.

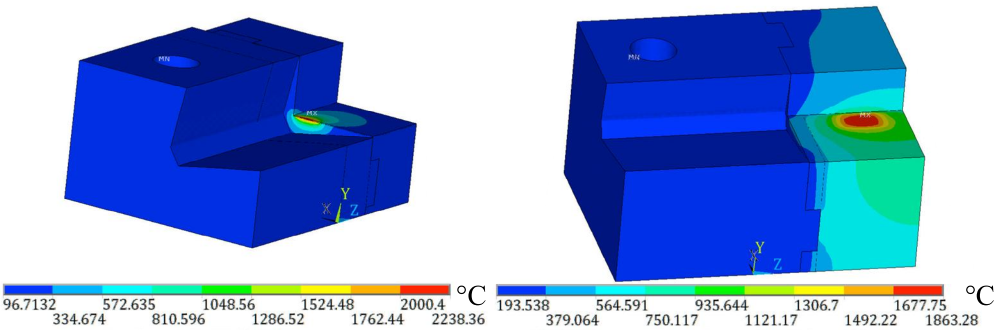

(a) Conventional XY slit (b) HHR XY slit

Figure 9 Temperature distributions from nodal solutions.

4-Conclusion

The TCCs of both a conventional XY slit and an HHR front-end XY slit were examined by comparing experimental results with those of FEM analyses under various conditions. As a result, the minimum TCCs could be assumed to be at least greater than 150,000 $W\cdot m^{-2}\cdot K^{-1}$for the conventional type and 400,000 $W\cdot m^{-2}\cdot K^{-1}$for the HHR type at the actual assembling torque. The maximum temperatures of the Ta slits were calculated by applying the minimum TCCs. As a result, both types of XY slits were found to be operational, because the melting point of Ta is 3,000°C.

References

[1] M. Sano, S. Takahashi, T. Mochizuki, A. Watanabe, M. Oura and H. Kitamura, Quantitative estimation of thermal contact conductance of a real front-end component at SPring-8 fromt-ends, Jorunal of Synchrotron RadiationVol. 15(2008) 1-7.